Design of an ultra-low power MFSK system in the presence of jamming

Yi Xiang
ECE department
University of California, San Diego
La Jolla, USA
y9xiang@ucsd.edu

Laurence Milstein
ECE department
University of California, San Diego
La Jolla, USA
milstein@ece.ucsd.edu

MILCOM 2021 - 2021 IEEE Military Communications Conference (MILCOM) | 978-1-6654-3956-5/21/$31.00 ©2021 IEEE | DOI: 10.1109/MILCOM52596.2021.9653041

***Abstract*—We are interested in a communication system that operates in a jamming environment under stringent power constraints, but is flexible with bandwidth constraints. Our approach is to consider some of the key elements in a transceiver and optimize them for low power consumption. An obvious consequence of this is that high complexity components of the system, such as matched filters, forward error correction (FEC) that employs iterative decoders, coherent demodulators, and bandwidth-efficient modulation formats, are not feasible for this research. Rather, our system is designed using M-ary FSK with non-coherent detection and fast frequency hopping (FFH), optimized two-pole bandpass filters (BPF), and Reed-Solomon (RS) codes with hard-decision decoding. Among other things, we show that by properly optimizing the key parameters of the BPFs and RS codes, we can design the system to be significantly less complex than an optimal one, and only lose at most 1.4 dB in terms of performance in most cases, compared to the conventional matched filter receiver.**

***Index Terms*—M-ary FSK, multipath fading, ultra-low power-consumption, non-coherent detection, low-complexity filtering, fast frequency-hopping, partial-band noise jamming.**

I. Introduction

Frequency-hopping (FH) is widely used in military communication systems. In particular, fast FH with M-ary FSK (FFH-MFSK) is a typical non-coherent communication scheme.Among the intelligent jamming strategies are partial-band noise jamming (PBJ) and multi-tone jamming (MTJ). Attempts have been made to study and combat various intelligent jammers and interferences in different channel conditions with appropriate signal selection and error-correction coding [1]–[6]. The combined effects of diversity and coding to combat multi-tone jamming in a Rayleigh fading channel are studied in [1]; a new multi-user receiver based on equal gain combining and maximum likelihood (ML) detection is proposed in [2], where the new detector is found to have significantly less computational complexity than the traditional ML detector with an acceptable performance degradation; the performance of an optimal ML receiver in partial-band noise jamming and frequency-selective Rician fading channels is derived in [4]; the composite effect of multi-tone jamming and partial-band noise jamming in a Rayleigh fading channel with time and frequency offsets is analyzed in [5]; the performances of a FFH/MFSK system with various receivers in multi-tone jamming are compared in [6].

In [7], we addressed the design and performance analysis of an ultra-low power communications system. As a concrete example of constraints that ultra-low power consumption impose on system design such as in [7], consider a scenario whereby the maximum total power consumption (transmission power and circuit power) was limited to 1mW, the data rate had to be at least 100kb/sec, the distance between the transmitter and receiver had to be at least 1 km, and the uncoded bit error rate (BER) could not exceed 0.001, over an AWGN channel [8]. If an attempt is made to implement this system with a coherent receiver, a phase-lock loop (PLL) is needed to achieve phase and frequency synchronization. However, from [9], it is shown that the minimum power consumption of a well-designed PLL is on the order of 550 microwatts. In other words, the PLL alone consumes more than 50% of the total power-consumption budget. Thus, in [7], power-hungry components, such as matched filters, were replaced with 2-pole BPFs, soft-decision iterative decoders were replaced by hard-decision decoders, etc. What we found was that if these ad-hoc components were locally optimized, significant reductions in power consumption could be achieved with relatively small increase in BER.

However, what was missing from [7] was the presence of intelligent jammers. As a consequence, in this paper, we add the presence of a partial-band jammer that maximizes the amount of performance degradation, and we revise our system design to include fast-frequency hopping (FFH).

The demodulator consists of a parallel bank of M branches, each with a BPF whose center frequency is the frequency of the corresponding tone, followed by a square-law detector, a sampler that takes L samples of a symbol, and an adder that computes the sum of the L samples. We choose the largest among the M test statistics to make a decision. As a point of comparison, this structure, if used with matched filters, is a conventional design of an FFH-MFSK demodulator [10] – [14].

In Section II, we analyze the performance of an FFH-MFSK receiver in full-band noise jamming, whereby we compare matched filter and 2-pole BPF detection, in both a non-fading channel and a slow, flat Rician fading channel. We enhance

This research was supported in part by the Office of Naval Research under grant number: N00014-17-2299, and grant number N00014-21-1–2470.

the performance with diversity and/or coding and compare the performance. In Section III, we compare the performance of an FFH-MFSK receiver in PBJ with matched filter and 2-pole BPF detection. For the matched filter case, we find the worst-case performance, and for the 2-pole BPF case, we find the Nash Equilibrium (NE) [15] at a given probability of error (10^{-3}), i.e., neither the system can benefit from changing the time-bandwidth parameter, z, nor can the jammer benefit from changing the fraction to jam, ρ. In Section IV, we present numerical results.

II. Demodulator Performance in Full-band Jamming

In this section, we analyze the performance of an FFH-MFSK non-coherent demodulator in full-band noise jamming. Although full-band jamming is simplistic and an intelligent jammer would rarely use it, the analysis in this section serves as a basis so that we can easily generalize it to PBJ in later sections. The block diagram of an FFH-MFSK non-coherent demodulator is shown in Fig. 1 [10] – [14], where the received dehopped waveform, $\underline{r}(t)$, is given by

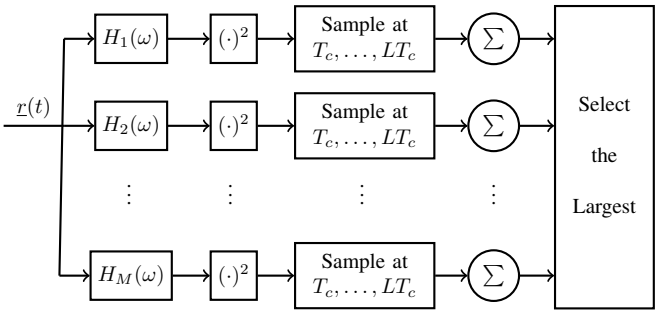

Fig. 1. FFH-MFSK non-coherent demodulator structure

$$\underline{r}(t) = s(t) + \underline{n}_w(t) + \underline{n}_J(t). \tag{1}$$

In (1), $s(t)$ is the dehopped FSK signal, $\underline{n}_w(t)$ is thermal noise with single-sided power spectral density N_0, and $\underline{n}_J(t)$ is broadband noise by the jammer with single-sided power spectral density N_J. Also, T_c is the hop duration, $L \geqslant 1$ is the number of hops/symbol, and $(\cdot)^2$ denotes square law detection. A decision is made by selecting the largest of the M outputs of the adders. The filters are either matched filters or 2-pole BPFs. The transfer function and corresponding impulse response of the i^{th} 2-pole BPF are given by

$$\begin{aligned} H_i(s) &= \frac{2\pi W s}{s^2 + 2\pi W s + (2\pi f_i)^2} \quad i = 1, 2, \ldots, M, \\ h_i(t) &= 2\pi W e^{-\pi W t} \cos(2\pi f_i t) u(t) \quad i = 1, 2, \ldots, M, \end{aligned} \tag{2}$$

respectively, where W is the filter bandwidth and $\Delta f \triangleq f_2 - f_1 = 1/T_c$ is the tone spacing, i.e., we use the minimum tone spacing that satisfies orthogonal signaling, since the optimal performance we found in [7] was almost always achieved with this tone spacing. We assumed $f_i \gg W, \forall i$ when we derived the impulse response from the transfer function. We optimize the time-bandwidth parameter $z \triangleq WT_c$ to minimize the signal-to-jamming power ratio (E_b/N_J) required to reach a given BER for the 2-pole BPF system and compare the results to the corresponding matched filter system.

We will ignore thermal noise in the following analysis in deference to the typically dominant jamming power, as is done in the references such as [10], [16], [17].

A. Matched Filter Detection

The symbol error rate (SER) of an FFH-MFSK-MF system in full-band jamming, $P_{s,MF}$, is given in [10]. In a slow, flat Rician fading channel, the symbol amplitude $\underline{R}$ is Rician distributed:

$$f_{\underline{R}}(r) = \frac{r}{\sigma^2} e^{-\frac{A^2+r^2}{2\sigma^2}} I_0\left(\frac{Ar}{\sigma^2}\right). \tag{3}$$

If we let γ denote the $E_s/N_J = (\log_2 M)E_b/N_J$ without fading, and $\bar{\gamma}$ denote the average $E_s/N_J = (\log_2 M)E_b/N_J$ with Rician fading, the pdf of γ is given by [18]

$$f(\gamma) = \frac{(1+K)e^{-K}}{\bar{\gamma}} e^{-\frac{(1+K)\gamma}{\bar{\gamma}}} I_0\left(\sqrt{4K(1+K)\frac{\gamma}{\bar{\gamma}}}\right), \tag{4}$$

where K is the Rician K-factor defined as $K \triangleq \frac{A^2}{2\sigma^2}$.

Combining (3) and (4), the symbol error rate (SER) for an FFH-MFSK-MF system in the presence of full-band noise jamming and slow, flat Rician fading as a function of the average E_s/N_J and the Rician K-factor is given by

$$\begin{aligned} P_{s,MF-Rice} &= \int_0^\infty P_{s,MF} \cdot f(\gamma) d\gamma \\ &= \int_0^\infty \frac{(1+K)e^{-K}}{\bar{\gamma}} e^{-\frac{(1+K)\gamma}{\bar{\gamma}}} I_0\left(\sqrt{4K(1+K)\frac{\gamma}{\bar{\gamma}}}\right) \\ &\left[1 - \int_0^\infty \left(1 - e^{-v} \sum_{k=0}^{L-1} \frac{v^k}{k!}\right)^{M-1} \left(\frac{v}{\gamma}\right)^{\frac{L-1}{2}} e^{-(\gamma+v)} I_{L-1}(2\sqrt{\gamma v}) dv\right] d\gamma \\ &= 1 - \int_0^\infty \int_0^\infty \frac{(1+K)e^{-K}}{\bar{\gamma}} e^{-\frac{(1+K)\gamma}{\bar{\gamma}}} I_0\left(\sqrt{4K(1+K)\frac{\gamma}{\bar{\gamma}}}\right) \\ &\left(1 - e^{-v} \sum_{k=0}^{L-1} \frac{v^k}{k!}\right)^{M-1} \left(\frac{v}{\gamma}\right)^{\frac{L-1}{2}} e^{-(\gamma+v)} I_{L-1}(2\sqrt{\gamma v}) dv d\gamma. \end{aligned} \tag{5}$$

Numerical results for $M = 16, L = 2$ with both no fading and Rician ($K = 10$) fading, are presented in Section IV.

B. Two-pole BPF Detection

One problem with 2-pole BPF detection is that there exists both inter-carrier interference (ICI) and inter-symbol interference (ISI), where ISI in principal comes from all previous pulses. However, as discussed in more detail in [7], significant ISI primarily comes from the previous pulse so we only consider that pulse as the source of ISI. Let Ps_{in}^m denote the probability that the current symbol is at frequency f_i but is detected as $f_n, n \neq i$, and where the previous symbol is at frequency f_m. The union bound on the average SER is

$$\bar{P}_{s,2pole} = \frac{1}{M^2} \sum_{i=1}^{M} \sum_{n=1, n\neq i}^{M} \sum_{m=1}^{M} Ps_{in}^m, \tag{6}$$

where Ps_{in}^{m} can be evaluated numerically, as shown in [19]. The union bound on the SER in full-band noise jamming and slow, flat Rician fading with 2-pole BPF detection is given by

$$\bar{P}_{s,2pole-Rice} = \int_0^\infty \bar{P}_{s,2pole} \cdot f(\gamma) d\gamma. \tag{7}$$

Table I lists the optimal time-bandwidth parameter, z, along with the optimal performance of our ad-hoc receiver in comparison with the matched filter system performance for $M = 2$ and 16, $L = 2$, and $K = \infty, 10$ and 0, where the optimization is done using an exhaustive search, as discussed in more detail in [7].

The numerical results for $M = 16$ and $L = 2$ with both no fading and Rician fading are presented in Section IV.

C. Demodulator Performance with Diversity

With the assumption that the fade is slow, all hops of a symbol have the same amplitude, making the system vulnerable to deep fades. Diversity can be achieved by interleaving the hops and thus randomizing hop amplitudes. We assume perfect interleavers (i.e., infinitely long) are used so that the hop amplitudes are i.i.d.. However, note that if the channel is frequency selective fading instead of flat, then fast frequency hopping has the potential to yield frequency diversity, and thus there would be no need for the interleavers.

The detailed analyses to find the union bound on error rate for both matched filter and 2-pole BPF detection are shown in [19]. An exception is, when the channel experiences Rayleigh fading, and matched filters are used for detection, the exact symbol error rate is given in [10]. The optimal time-bandwidth parameter z, and the optimal performance in comparison with the MF performance, are listed in Table I, and the numerical results for $M = 16$ and $L = 2$ with both no fading and Rician ($K = 10$) fading, are presented in Section IV.

TABLE I
OPTIMAL PARAMETER AND E_b/N_J @ $P_b = 10^{-3}$

		Without diversity			With diversity		
M	K	z_{opt}	2-pole	MF	z_{opt}	2-pole	MF
2	∞	0.60	13.0 dB	11.6 dB	0.60	13.0 dB	11.6 dB
	10	0.56	16.2 dB	15.0 dB	0.64	14.4 dB	13.0 dB
	0	0.52	31.9 dB	31.0 dB	0.84	22.0 dB	20.2 dB
16	∞	0.56	8.0 dB	6.7 dB	0.56	8.0 dB	6.7 dB
	10	0.48	12.0 dB	10.6 dB	0.56	9.6 dB	8.5 dB
	0	0.44	28.2 dB	27.4 dB	0.72	18.0 dB	16.2 dB

D. Demodulator Performance with RS Coding

The choice of RS codes with hard decision decoding here is particularly appropriate because of the lower complexity compared to, say, soft decision in general, and iterative decoding, in particular, and the straightforward manner in which the RS encoded codewords can be mapped to the MFSK signal set. We optimize for the suboptimal system the code dimension k in conjunction with the time-bandwidth parameter z for MFSK with (n, k) RS codes. We fixed the code length and exhaustively searched all possible values of code dimension, k, to find the k that minimizes the E_b/N_J required at $P_b = 10^{-3}$. For any case analyzed in previous sections, the BER for the coded system is given by [10]

$$P_{coded} = \frac{n+1}{2n} \cdot \frac{1}{n} \sum_{i=t+1}^{n} i \binom{n}{i} P_{uncoded}^{i} (1 - P_{uncoded})^{n-i}, \tag{8}$$

where $P_{uncoded}$ is the uncoded RS SER related to the MFSK SER P_s by

$$\begin{aligned} P_{uncoded} &= 1 - (1 - P_s)^{\frac{\log_2(n+1)}{\log_2 M}}, \\ k &= 1, 3, \ldots, n-2, \quad t = \frac{n-k}{2}, \end{aligned} \tag{9}$$

and $n = M^x - 1$ for some positive integer x, i.e., x MFSK symbol per RS symbol. The optimal k and z along with performance in comparison with the matched filter system for $M = 16$, are listed in Table II. Numerical results of systems employing FEC are presented in Section IV.

TABLE II
OPTIMAL PARAMETER AND E_b/N_J @ $P_b = 10^{-3}$

n	k_{MF}	k_{2pole}	K	diversity	z_{opt}	2-pole	MF
15	9	9	10	No	0.48	9.0 dB	7.9 dB
255	181	173	10	No	0.48	8.1 dB	7.1 dB
15	11	11	10	Yes	0.52	8.2 dB	7.2 dB
15	5	5	0	No	0.44	15.0 dB	13.8 dB
255	109	113	0	No	0.44	13.8 dB	12.6 dB
15	7	7	0	Yes	0.56	11.5 dB	10.3 dB

III. Demodulator Performance in Partial-band Noise Jamming

The previous section focused on full-band noise jamming, where the jammer jams the entire spread spectrum bandwidth. In reality, the jammer may select to jam a fraction (ρ) of the spread spectrum in order to optimize the effect on the communication system, i.e., to maximize the BER at some E_b/N_J. In this section, we consider partial-band jamming with an FFH-MFSK system using either matched filter or 2-pole BPF detection. To be specific, for the matched filter system, we find the worst-case performance, and for the 2-pole BPF system, we find the NE at a given BER.

Suppose the partial-band interference is a zero-mean Gaussian random process with a flat power spectral density over a fraction ρ of the total spread spectrum bandwidth and zero elsewhere (and thus the demodulation is error-free with probability $1 - \rho$). That is, a fraction of the total spread spectrum bandwidth W_{ss}, $W_J = \rho W_{ss}$ is jammed. Furthermore, as is common in the literature, we assume that, on a given hop, each M-ary band lies either entirely inside or entirely outside W_J [16]. In the region or regions where the power spectral density is nonzero, its value is N_J/ρ.

As is discussed in more details in the [19], thermal noise has little effects on performance so we will continue ignoring it in this section.

A. Matched Filter Detection

In this section, we find the worst-case partial-band jamming performance, both in a non-fading channel and in a slow, flat Rician fading channel.

1) Non-fading channel: In a non-fading channel, the performance in full-band noise jamming was derived in [10], and thus with the aforementioned assumptions, the SER in partial-band noise jamming is given by

$$P_s(\rho) = \rho\Big[1 - \int_0^\infty \Big(1 - e^{-v}\sum_{k=0}^{L-1}\frac{v^k}{k!}\Big)^{M-1}\Big(\frac{v}{\rho\gamma}\Big)^{\frac{L-1}{2}} e^{-(\rho\gamma+v)} I_{L-1}(2\sqrt{\rho\gamma v})dv\Big], \tag{10}$$

where $\gamma = (\log_2 M)\frac{E_b}{N_J}$. The worst-case performance in PBJ, found by differentiating $P_s(\rho)$ and setting it to zero, is given in [16] for $L = 1$, and in this paper, we extend the results to $L > 1$:

$$P_{b,worst} = \begin{cases} P_b(\rho = 1), & \frac{E_b}{N_J} \leqslant \gamma_0, \rho_{worst} = 1, \\ \frac{\beta_b}{E_b/N_J}, & \frac{E_b}{N_J} > \gamma_0, \rho_{worst} = \frac{\gamma_0}{E_b/N_J}, \end{cases} \tag{11}$$

and thus the fraction ρ_{worst} at the BER P_b^* is given by

$$\rho_{worst} = \frac{\gamma_0}{\beta_b} \cdot P_b^* \tag{12}$$

The values of γ_0 and β_b for $M = 2, 4, 8, 16, 32$ and $L = 1, 2, 3, 4, 5, 6, 7$ are shown in Table III, and detailed analysis is shown in [19]. Note that, for the special case of $L = 1$, the values of γ_0 and β_b can also be found in [16], [17].

TABLE III
VALUES OF γ_0 (DB) AND β_b FOR A NON-FADING CHANNEL

	L \ M	1	2	3	4	5	6	7
γ_0	2	3.01	3.93	4.50	4.93	5.27	5.56	5.80
	4	0.76	1.65	2.21	2.62	2.96	3.24	3.48
	8	-0.33	0.53	1.07	1.48	1.81	2.09	2.33
	16	-0.98	-0.15	0.38	0.78	1.10	1.38	1.61
	32	-1.41	-0.61	-0.09	0.30	0.62	0.89	1.12
β_b	2	0.368	0.470	0.548	0.613	0.670	0.721	0.768
	4	0.233	0.300	0.350	0.391	0.428	0.461	0.491
	8	0.195	0.251	0.292	0.326	0.357	0.384	0.409
	16	0.181	0.231	0.268	0.299	0.326	0.351	0.373
	32	0.176	0.222	0.257	0.286	0.311	0.334	0.356

2) Slow, flat Rician fading chanel: In a Rician fading channel, the demodulator performance in full-band noise jamming was given in (5). and thus the average symbol error rate in partial-band noise jamming is given by

$$P_s(\rho) = \rho - \int_0^\infty\int_0^\infty \frac{(1+K)e^{-K}}{\bar{\gamma}} e^{-\frac{(1+K)\gamma}{\rho\bar{\gamma}}} I_0\Big(\sqrt{4K(1+K)\frac{\gamma}{\rho\bar{\gamma}}}\Big) \Big(1 - e^{-v}\sum_{k=0}^{L-1}\frac{v^k}{k!}\Big)^{M-1}\Big(\frac{v}{\gamma}\Big)^{\frac{L-1}{2}} e^{-(\gamma+v)} I_{L-1}(2\sqrt{\gamma v})dvd\gamma, \tag{13}$$

where $\gamma = (\log_2 M)\frac{E_b}{N_J}$. The worst-case partial-band jamming performance is again found by differentiating $P_s(\rho)$ and setting it to zero, and it takes the same form as (11). The values of γ_0 and β_b for $M = 2, 4, 8, 16, 32$ and $L = 1, 2, 3, 4, 5, 6, 7$ are shown in Table IV, and detailed analysis is shown in [19]. The numerical results for worst-case performance in PBJ for $M = 16, L = 2, K = 10$ are shown in Fig. 6. Note that, for $M = 2$ and $L = 1$, the values of γ_0 and β_b can also be found in [20].

TABLE IV
VALUES OF γ_0 (DB) AND β_b FOR A SLOW, FLAT RICIAN FADING CHANNEL

	L \ M	1	2	3	4	5	6	7
γ_0	2	3.88	4.77	5.32	5.73	6.07	6.35	6.58
	4	1.58	2.43	2.98	3.37	3.71	3.98	4.20
	8	0.46	1.28	1.80	2.20	2.50	2.79	3.02
	16	-0.23	0.56	1.07	1.45	1.77	2.04	2.24
	32	-0.69	0.06	0.57	0.94	1.25	1.49	1.72
β_b	2	0.405	0.514	0.597	0.667	0.728	0.783	0.833
	4	0.254	0.325	0.377	0.421	0.460	0.494	0.526
	8	0.211	0.269	0.312	0.347	0.379	0.407	0.433
	16	0.194	0.245	0.283	0.315	0.343	0.368	0.391
	32	0.186	0.233	0.269	0.298	0.324	0.347	0.368

B. Two-pole BPF Detection

For the 2-pole BPF system, there is a jamming game between the system and the jammer. Each player takes turns to optimize its strategy until a NE is reached. To be specific, the system optimizes the time-bandwidth parameter, z, to minimize the E_b/N_J required to reach the BER of 10^{-3}, while the jammer optimizes the fraction to jam, ρ, to maximize it. With an arbitrary initial condition, the two players iteratively optimize their strategies until a NE is reached. The performance at NE for $M = 16, L = 2$, in a Rician ($K = 10$) fading channel, is presented in Section IV, and the parameter pair (z, ρ) at BER = 10^{-3} is summarized in Table. V.

TABLE V
PARAMETER PAIR (z, ρ) AT NE AT BER = 10^{-3}

K \ M	2	16
∞	$(0.45, 5.5 \times 10^{-3})$	$(0.48, 4.4 \times 10^{-3})$
10	$(0.46, 6.1 \times 10^{-3})$	$(0.48, 4.8 \times 10^{-3})$

Note that the optimal ρ for matched filter detection can be found using (12) and Tables III and IV. The numerical results are $\rho = 5.3 \times 10^{-3}$ for $M = 2$ and $K = \infty$, $\rho = 4.2 \times 10^{-3}$ for $M = 16$ and $K = \infty$, $\rho = 5.8 \times 10^{-3}$ for $M = 2$ and $K = 10$ and $\rho = 4.6 \times 10^{-3}$ for $M = 16$ and $K = 10$. The optimal ρ for matched filter detection (listed in this paragraph) and 2-pole BPF detection (listed in Table V) can be seen to be quite similar.

IV. NUMERICAL RESULTS

We present numerical results for the scenarios evaluated in previous sections. In all the figures of this section, $M = 16, L = 2, K = 10$, and when FEC is used, $n = 15$. We use simulations to support analyses, where the simulation result (shown in markers) corresponds to the analytical result (shown in lines) whose legend is directly above it.

Figure 2 shows the performance analysis and simulation results with matched filter and 2-pole BPF detection both with Rician fading and without fading, and with and without diversity. Figs. 3 and 4 show the performance with optimal RS codes in a Rician fading channel, without and with diversity, respectively. Fig. 5 shows the performance comparison for $K = 0, 10, \infty$, with and without coding and/or diversity.

Figure 6 shows the results in partial-band jamming in a Rician fading channel. With matched filter detection, the worst-case performance is shown, and with 2-pole BPF detection, the performance curves at the NE are shown. The solid and dashed gray lines are the performances in full-band and partial-band ($\rho = 4.6 \times 10^{-3}$) jamming, respectively. The gray dotted line is the worst-case jamming performance and is tangent to the gray dashed line at BER = 10^{-3}. The solid and dashed black lines are the performances of the same system and channel, but with 2-pole BPF detection with full-band and partial-band ($\rho = 4.8 \times 10^{-3}$) jamming, and the circular and triangular markers are the corresponding simulations, respectively.

Note that the partial-band jamming curve "flattens out" at low E_b/N_J, and this is because, at the target BER of 10^{-3}, the jammer's optimal fraction of the total bandwidth to jam is very small. As a consequence, it is likely that a given symbol is not jammed, so that the average error rate is low. For the MF system, the optimal fraction is computed using Equation (19), and for the 2-pole BPF system, it is found by iteratively optimizing the parameter of each player (system and jammer) until an NE is reached. Note that the optimal fractions for both systems (MF and 2-pole) turn out similar.

As shown in Fig. 5, both coding and diversity combining are useful ways of combatting fading channels, especially Rayleigh fading channels. However, the use of coding in conjunction with diversity combining does not result in a large additional performance gain compared to only one of them being used, especially for a Rician ($K = 10$) fading channel.

To be specific, with full-band noise jamming, the performance degradation is 1.8 dB when we use diversity combining in a Rayleigh fading channel, and in other cases, the performance degradation is between 1.0 dB and 1.4 dB, which is consistent with what we found in [7]. With partial-band noise jamming. The performance degradation is between 0.8 dB and 0.9 dB, and the advantage of using 16FSK instead of BFSK is about 3dB at the NE when the BER is 10^{-3}.

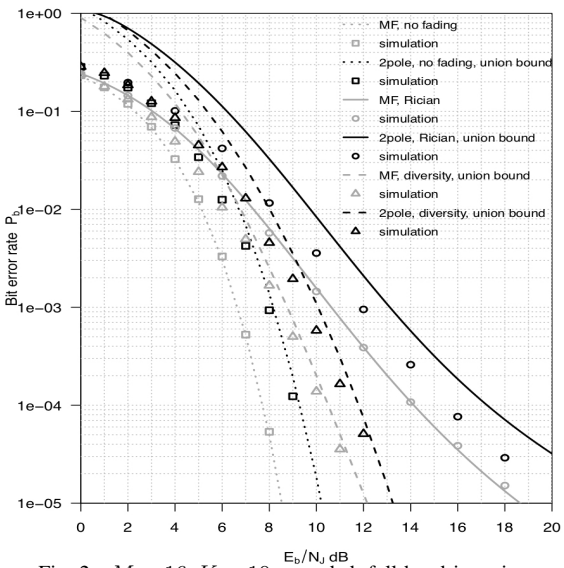

Fig. 2. $M = 16, K = 10$, uncoded, full-band jamming.

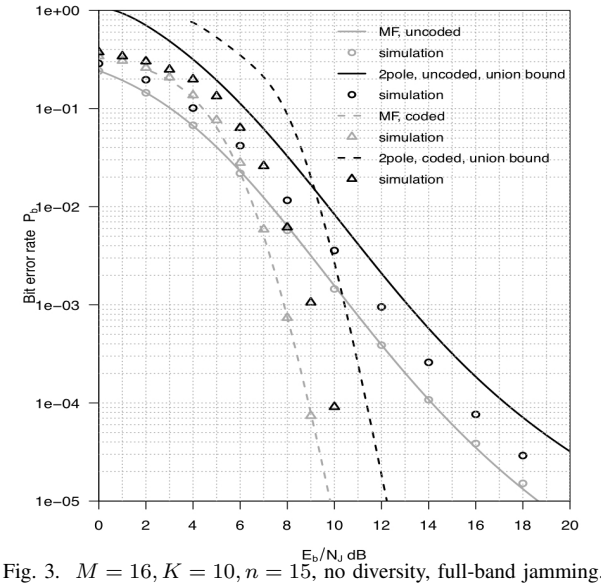

Fig. 3. $M = 16, K = 10, n = 15$, no diversity, full-band jamming.

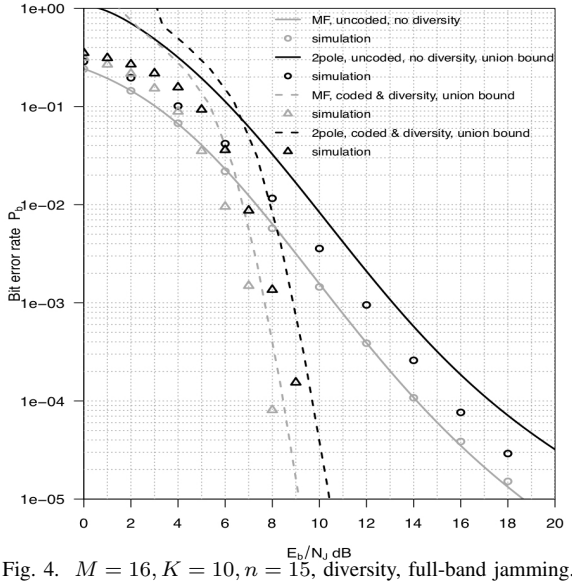

Fig. 4. $M = 16, K = 10, n = 15$, diversity, full-band jamming.

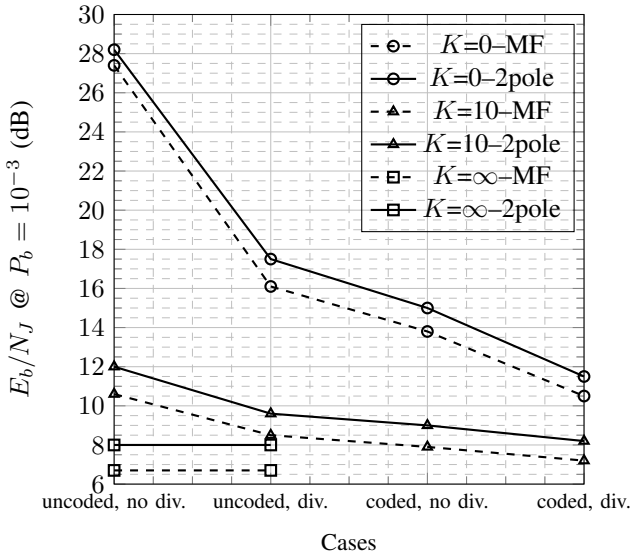

Fig. 5. Performance comparison in full-band jamming.

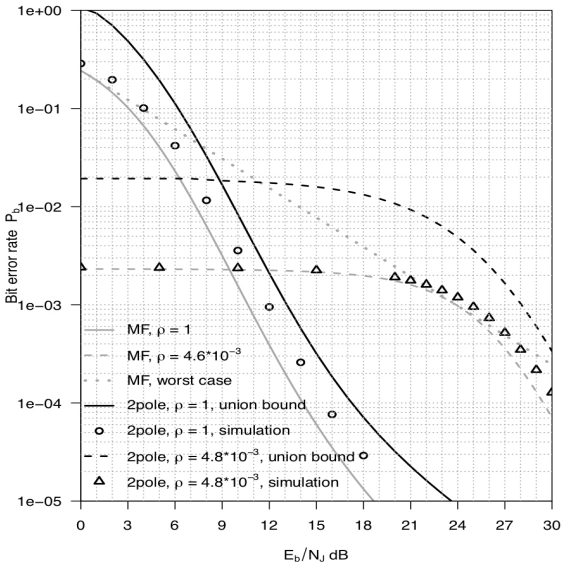

Fig. 6. NE, $M = 16, K = 10$, partial and full-band jamming.

V. Conclusion

This work can be considered as an extension of [7]. The essence is the use of a spectrally-inefficient, but power-efficient, waveform, in conjunction with low complexity filtering and demodulation. The goal was to minimize transmission energy, subject to a predetermined average probability of error, in a jamming environment. Hence we chose non-coherent MFSK instead of coherent MQAM, we chose RS encoding with hard-decision decoding instead of soft-decision iterative decoding for a capacity-approaching code, and we chose simple two-pole bandpass filters instead of matched filters.

We specifically compared the performance of an FFH-MFSK non-coherent receiver when matched filters are replaced by 2-pole BPFs, for non-fading, Rayleigh, and Rician fading (K=10) channels. We further considered a coded system with RS codes and hard-decision decoding for various cases. For PBJ, we found the worst-case performance of a FFH-MFSK system with matched filter detection, and also the NE with 2-pole BPF detection. We found that by carefully optimizing the system parameters, such as filter bandwidth and code dimension, we could achieve the desired performance with a penalty in E_b/N_J of 0.8–1.8 dB compared to the more conventional design using non-coherent FSK with matched filter detection. Note that, with full-band noise jamming, the 1.8 dB performance degradation only occurs when diversity is used in a Rayleigh fading channel. In other cases, the penalty is between 1.0 dB and 1.4 dB, which is consistent with what we found in [7]. With partial-band noise jamming. The performance degradation is between 0.8 dB and 0.9 dB.

References

[1] Y. Liu, "Diversity-Combining and Error-Correction Coding for FFH/MFSK Systems over Rayleigh Fading Channels under Multitone Jamming," in *IEEE Transactions on Wireless Communications*, vol. 11, no. 2, pp. 771-779, February 2012, doi: 10.1109/TWC.2011.120911.110462.

[2] F. Yang, W. Xiong and J. Song, "Equal Gain Combining-Based Maximum Likelihood Detector for FFH/MFSK Systems," in *IEEE Communications Letters*, vol. 22, no. 7, pp. 1334-1337, July 2018, doi: 10.1109/LCOMM.2017.2687443.

[3] A. J. Al-Dweik and B. S. Sharif, "Exact Performance Analysis of Synchronous FH-MFSK Wireless Networks," in *IEEE Transactions on Vehicular Technology*, vol. 58, no. 7, pp. 3771-3776, Sept. 2009, doi: 10.1109/TVT.2009.2013471.

[4] J. Zhang, K. C. Teh and K. H. Li, "Error probability analysis of FFH/MFSK receivers over frequency-selective Rician-fading channels with partial-band-noise jamming," in *IEEE Transactions on Communications*, vol. 57, no. 10, pp. 2880-2885, October 2009, doi: 10.1109/TCOMM.2009.10.080114.

[5] L. Le, K. C. Teh and K. H. Li, "Jamming Rejection Using FFH/MFSK ML Receiver Over Fading Channels With the Presence of Timing and Frequency Offsets," in *IEEE Transactions on Information Forensics and Security*, vol. 8, no. 7, pp. 1195-1200, July 2013, doi: 10.1109/TIFS.2013.2264053.

[6] Y. Han and K. C. Teh, "Error probabilities and performance comparisons of various FFH/MFSK receivers with multitone jamming," in *IEEE Transactions on Communications*, vol. 53, no. 5, pp. 769-772, May 2005, doi: 10.1109/TCOMM.2005.847139.

[7] Y. Xiang and L. B. Milstein, "Design and Performance Analysis for Short Range, Very Low-Power Communications," in *IEEE Transactions on Communications*, vol. 68, no. 9, pp. 5938-5950, Sept. 2020, doi: 10.1109/TCOMM.2020.3005454.

[8] Ali Nikoofard, Hamed Abbasi Zadeh, Patrick P. Mercier, "A 0.6-mW 16-FSK Receiver Achieving a Sensitivity of âĹŠ103 dBm at 100 kb/s", *Solid-State Circuits IEEE Journal of*, vol. 56, no. 4, pp. 1299-1309, 2021.

[9] H. R. Kooshkaki, P. P. Mercier, "A 0.55mW Fractional-N PLL with a DC-DC Powered Class-D VCO Achieving Better than -66dBc Fractional and Reference Spurs for NB-IoT," in Proc. *IEEE Custom Integrated Circuits Conference (CICC)*, Mar. 2020.

[10] J. Proakis and M. Salehi, *Digital Communications*, fifth edition.

[11] H. Ma and M. Poole, "Error-Correcting Codes Against the Worst-Case Partial-Band Jammer," in *IEEE Transactions on Communications*, vol. 32, no. 2, pp. 124-133, February 1984, doi: 10.1109/TCOM.1984.1096036.

[12] J. Wang and M. Moeneclaey, "Multiple hops/symbol FFH-SSMA with MFSK modulation and Reed-Solomon coding for indoor radio," in *IEEE Transactions on Communications*, vol. 41, no. 5, pp. 793-801, May 1993, doi: 10.1109/26.225494.

[13] R. Viswanathan and K. Taghizadeh, "Diversity combining in FH/BFSK systems to combat partial band jamming," in *IEEE Transactions on Communications*, vol. 36, no. 9, pp. 1062-1069, Sept. 1988, doi: 10.1109/26.7518.

[14] R. C. Robertson and Kang Yeun Lee, "Performance of fast frequency-hopped MFSK receivers with linear and self-normalization combining in a Rician fading channel with partial-band interference," in *IEEE Journal on Selected Areas in Communications*, vol. 10, no. 4, pp. 731-741, May 1992, doi: 10.1109/49.136068.

[15] K. Binmore, 2007, *Game theory a very short introduction*, Oxford University Press.

[16] M. K. Simon, J. K. Omura, R. A. Scholtz and B. K. Levitt, *Spread Spectrum Communications Handbook*

[17] R. E. Ziemer and R. L. Peterson, *Digital Communications and Spread Spectrum Systems*, New York:Macmillan Publishing Company, 1985.

[18] M. K. Simon and M.-S. Alouini, *Digital Communication over Fading Channels*, vol. 95. John Wiley & Sons, 2005.

[19] Y. Xiang and L. B. Milstein, "On the use of FFH-MFSK for ultra-low power communications", in preparation.

[20] A. A. Ali, "Worst-case partial-band noise jamming of Rician fading channels," in *IEEE Transactions on Communications*, vol. 44, no. 6, pp. 660-662, June 1996, doi: 10.1109/26.506381.

[21] M Schwartz, W Bennett and S Stein, *Communication Systems and Techniques*, McGraw-Hill, 1966.